

UV excitation properties of Eu^{3+} at the S_6 site in bulk and nanocrystalline cubic Y_2O_3

Mingli Jia^a, Jiahua Zhang^{a,*}, Shaozhe Lu^a, Jiangting Sun^a, Yongshi Luo^a,
Xinguang Ren^a, Hongwei Song^a, Xiao-jun Wang^{a,b}

^a Key Laboratory of Excited State Processes, Changchun Institute of Optics, Fine Mechanics and Physics,
Chinese Academy of Sciences, Changchun 130033, PR China

^b Department of Physics, Georgia Southern University, Statesboro, GA 30460, USA

Received 8 September 2003; in final form 10 November 2003

Abstract

Increases of emission intensities for Eu^{3+} at the S_6 site relative to that at the C_2 site have been observed as UV excitation wavelength decreases from 300 to 200 nm in both bulk and nanocrystalline cubic $\text{Y}_2\text{O}_3:\text{Eu}^{3+}$. Analysis of excitation spectra suggests that the energy transfer from the host prefers to the S_6 site. In addition, spectral red-shift has been found in both charge transfer bands in nanocrystalline $\text{Y}_2\text{O}_3:\text{Eu}^{3+}$ compared to the bulk material. The number ratio of S_6 sites to C_2 sites is also smaller in nanocrystalline $\text{Y}_2\text{O}_3:\text{Eu}^{3+}$ than that in the bulk one.

© 2003 Elsevier B.V. All rights reserved.

1. Introduction

Trivalent europium-activated Y_2O_3 ($\text{Y}_2\text{O}_3:\text{Eu}^{3+}$) has attracted much attention as a red emitting phosphor for commercial application on fluorescent lighting and displaying [1,2]. With the fast development of nanotechnology, the optical properties of nanocrystalline (NC) $\text{Y}_2\text{O}_3:\text{Eu}^{3+}$ have also been investigated extensively [3–11] for its potential applications on high resolution imaging and fundamental research, such as local environment probing [4] using the high sensitivity of Eu^{3+} ions to their surroundings.

It is well known that $\text{Y}_2\text{O}_3:\text{Eu}^{3+}$ phosphor absorbs UV light through a charge transfer band (CTB) or host excitation band and then yields red fluorescence peaking at 611 nm. There exist two types of crystallographic sites in cubic Y_2O_3 , S_6 and C_2 sites. The S_6 site has inversion symmetry in which electric dipole transition is forbidden. Due to the absence of the inversion symmetry and the permission of electronic dipole transition, the C_2 site

makes dominant contribution to the 611 nm emission which corresponds to $^5\text{D}_0-^7\text{F}_2$ transition of Eu^{3+} ions. Hence, the observed CTB and host excitation band in the excitation spectra by monitoring $^5\text{D}_0-^7\text{F}_2$ transition are mainly from the Eu^{3+} ions at the C_2 site. Although the S_6 site has little contribution to the red fluorescence, it could still compete with the C_2 site for UV absorption. To our knowledge, there have been no reports on the UV excitation properties of the Eu^{3+} at S_6 site in either bulk or NC $\text{Y}_2\text{O}_3:\text{Eu}^{3+}$. The S_6 site allows the magnetic dipole transition $^5\text{D}_0-^7\text{F}_1$ of Eu^{3+} , which provides the possibility to study the UV excitation properties of the S_6 site. In this Letter, the UV excitation properties of the CTB and host excitation band for Eu^{3+} at the S_6 site are investigated for both bulk and NC $\text{Y}_2\text{O}_3:\text{Eu}^{3+}$ samples. Increases of emission intensities for Eu^{3+} at the S_6 site relative to that at the C_2 site have been observed as UV excitation wavelength decreases from 300 to 200 nm. Decomposition of excitation spectra shows that the CTB of Eu^{3+} at the S_6 site lies in the high-energy side of that at the C_2 site, resulting in that the energy transfer from the host prefers to the S_6 site. In addition, spectral red-shift has been found in both charge transfer bands in NC $\text{Y}_2\text{O}_3:\text{Eu}^{3+}$ compared to the bulk material. The

* Corresponding author.

E-mail address: zjiahua@public.cc.jl.cn (J. Zhang).

number ratio of S_6 sites to C_2 sites is also smaller in NC $Y_2O_3:Eu^{3+}$ than that in the bulk one.

2. Experiments

The NC $Y_2O_3:1\% Eu^{3+}$ was prepared by fast thermal decomposition of metal nitrate solution. In the preparation, $Y(NO_3)_3$ and $Eu(NO_3)_3$ were dissolved in de-ionized water and mixed in an appropriate ratio to form the precursor solution. The precursor solution was then condensed in porcelain crucible at $90^\circ C$ and was decomposed rapidly at $500^\circ C$ followed by a heat treatment at $500^\circ C$ for 1 h. The particle size was determined to be ~ 7 nm by transmission electron microscopy (TEM), as shown in Fig. 1. The bulk $Y_2O_3:1\% Eu^{3+}$ crystal powders was obtained by annealing the prepared nanoparticles at $1250^\circ C$ in air. The crystal size was determined to be $2\text{--}3\ \mu m$ by field-emission scanning electron microscopy (FESEM). All the samples were identified as cubic structure by X-ray diffraction. The optical spectra were recorded at room temperature by a Hitachi F-4500 fluorescence spectrometer using a Xe lamp as the excitation source.

3. Results and discussion

Fig. 2 shows the excitation spectra of the 611 nm emission in bulk crystal sample (solid line) and NC sample (dotted line), respectively. Both spectra in 200–300 nm region consist of two bands. The band peaking around 210 nm is related to the host excitation, i.e., electronic transitions from O 2p valence band to the Y (5d 6s) conduction band (Y_2O_3 host lattice absorption) [12]. In comparison with bulk sample, a blue-shift of the host excitation band in the NC $Y_2O_3:Eu^{3+}$ sample is clearly observed due to the quantum confinement effects [13]. The other band occurring around 240 nm is attributed to the CTB absorption of Eu^{3+} at the C_2 sites. A clear red-shift of the CTB in NC $Y_2O_3:Eu^{3+}$ is observed. It is believed to associate with the surface states

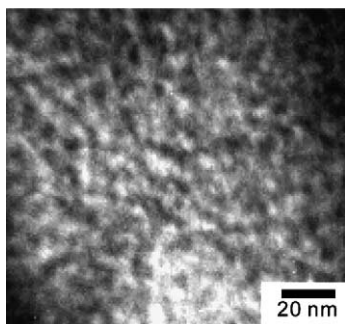


Fig. 1. TEM image of the $Y_2O_3:Eu^{3+}$ NC sample.

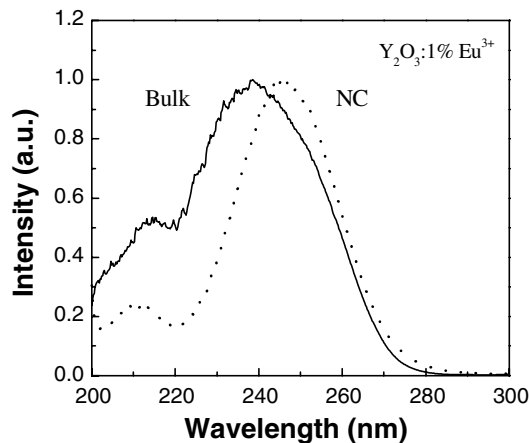


Fig. 2. Excitation spectra of the 611 nm emission in bulk sample (solid) and NC sample (dotted).

of the nanoparticles, which will be discussed in the following sections.

Figs. 3 and 4 show $^5D_0\text{--}^7F_J$ ($J = 0, 1, 2, 3$) emission spectra (solid) for bulk and NC samples, respectively, upon excitation of UV light with different wavelengths within 200 and 300 nm. The two emission lines located at 580 and 582 nm are focused, which originate from $^5D_0\text{--}^7F_0$ transition of Eu^{3+} at C_2 site and $^5D_0\text{--}^7F_1$ transition at S_6 site, respectively [5]. It is found that the intensity ratio of $^5D_0\text{--}^7F_1$ (S_6) to $^5D_0\text{--}^7F_0$ (C_2) emission line increases remarkably as the excitation wavelength decreases. This result suggests that the CTB of Eu^{3+} at the S_6 site locates at the high-energy side of Eu^{3+} at the C_2 site and the host prefers transferring excitation to the S_6 site. In fact, the different excitation wavelengths change the composition of the S_6 and C_2 spectral com-

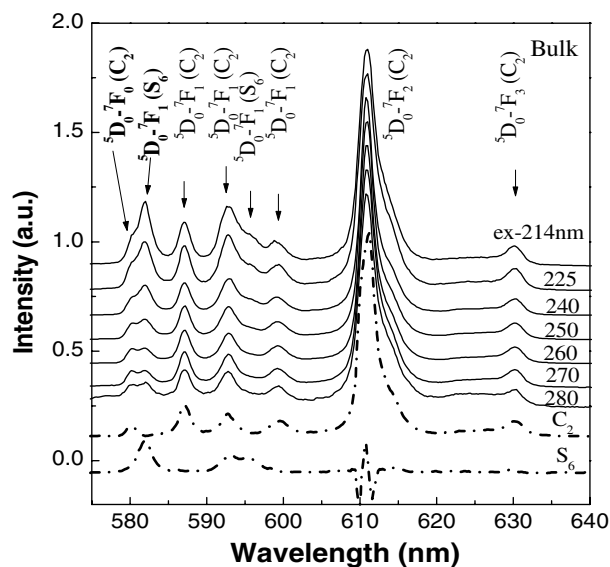


Fig. 3. Emission spectra of bulk sample excited by UV light with different wavelengths.

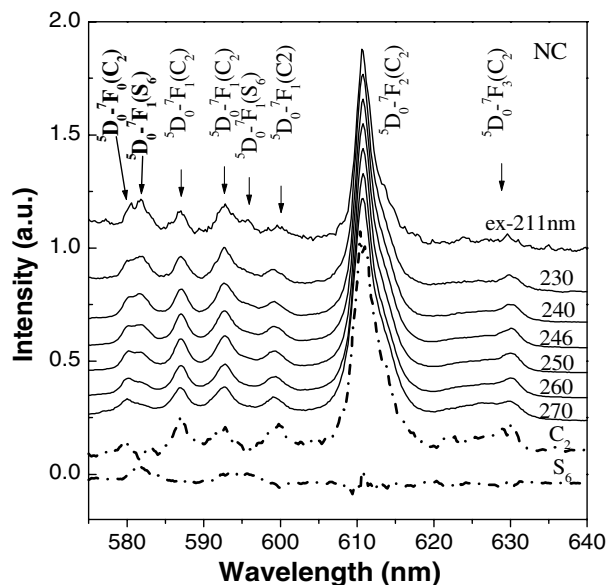


Fig. 4. Emission spectra of NC sample excited by UV light with different wavelengths.

ponents, which are deconvoluted and plotted on the bottom (dashed) in Figs. 3 and 4.

In order to obtain the excitation spectra of Eu^{3+} at S_6 site in UV region, excitation spectra were measured within 200 and 300 nm by collectively monitoring the ${}^5\text{D}_0\text{--}{}^7\text{F}_1$ (S_6) and ${}^5\text{D}_0\text{--}{}^7\text{F}_0$ (C_2) emissions. Fig. 5 depicts the excitation spectra for both bulk sample (curve 1, Fig. 5a) and NC sample (curve 1, Fig. 5b). As expected, the profiles of the excitation spectra are different from

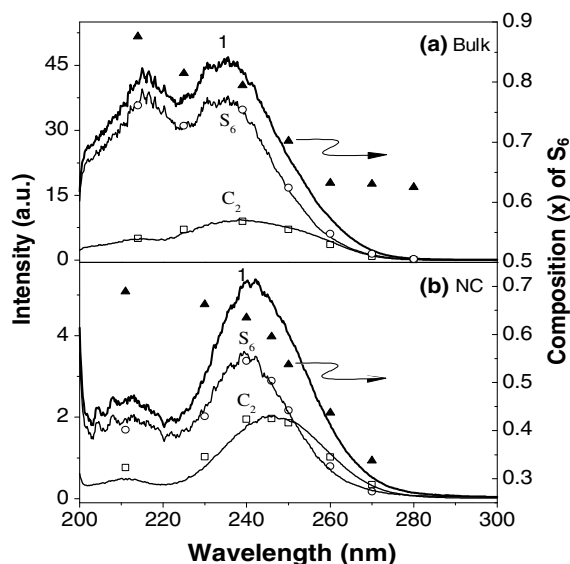


Fig. 5. Excitation spectra (curve 1) in UV region by collectively monitoring both 580 (${}^5\text{D}_0\text{--}{}^7\text{F}_0$) and 582 nm (${}^5\text{D}_0\text{--}{}^7\text{F}_1$) emissions for bulk sample (a) and NC sample (b), respectively. The spectral components for the S_6 and C_2 sites are resolved and presented below the curve 1 for each figure.

the ones presented in Fig. 2 for both bulk and NC samples, where the spectra correspond to the pure C_2 site only. It indicates that S_6 sites make an important contribution to the spectra. The spectral compositions from S_6 site, x , and from C_2 site, $(1-x)$, can be determined by deconvoluting the overlapped 580 (C_2) and 582 nm (S_6) emissions presented in Fig. 3 or Fig. 4. Using the profile of the excitation spectra in Fig. 2 as of pure C_2 site and scaling it to $(1-x)$, the excitation spectra of pure S_6 site in UV region is obtained by subtracting the rescaled excitation spectra of pure C_2 site from the curve 1.

The solid triangles (Fig. 5) indicate the change of spectral composition of S_6 site as a function of excitation wavelength. The open circles give the intensity of S_6 site obtained by multiplying curve 1 and the composition x . The open squares indicate the intensity of C_2 site obtained by multiplying curve 1 and $(1-x)$. Spectral deconvolution demonstrates that the CTB of the Eu^{3+} at the S_6 site lies in high-energy side of that at the C_2 site. This result might be related to the fact that S_6 site has inversion symmetry and shorter Y–O bond than C_2 site. The similar results have been reported in other Eu^{3+} -doped oxide hosts [14], where CTB positions exhibited a shift toward higher energy for VIII and XII coordination numbers of Eu^{3+} as bond length decreases. In our case, the cation Y^{3+} has VI coordination numbers in a pure phased cubic Y_2O_3 . It is also shown in Fig. 5 that CTBs of Eu^{3+} at both S_6 and C_2 sites have a spectral red-shift in NC $\text{Y}_2\text{O}_3:\text{Eu}^{3+}$, which has been observed by other investigators [5,10,11] and has been attributed to the larger Eu–O distance in nanomaterials [14]. The charge transfer state is related to stability of the electrons of the surrounding O^{2-} . In bulk materials, an O^{2-} ion is stabilized by surrounding positive ions. However, as particle size decreases to nanoscale, the surface-to-volume ratio of the particle increases and the degree of periodical disorder due to the surface structure increases, causing the electrons in O^{2-} less stable. As a result, it requires less energy to remove an electron from an O^{2-} ion; therefore, the energy levels of CTB are lowered.

In addition, as shown in Fig. 5, the intensity ratio of the host excitation band to the CTB of the S_6 site is greater than that of the C_2 site in both bulk and NC $\text{Y}_2\text{O}_3:\text{Eu}^{3+}$. It suggests that the host prefers transferring the excitation to the Eu^{3+} at S_6 site. The result could be attributed to the fact that the peak of the CTB of the S_6 site is closer to the host excitation band than that of the C_2 site. Moreover, in comparison with bulk $\text{Y}_2\text{O}_3:\text{Eu}^{3+}$, the integrated intensity of the S_6 site to that of the C_2 site decreases remarkably in NC sample, corresponding to the decrease of number ratio of the S_6 sites to the C_2 sites. It indicates that the local symmetry of Y_2O_3 lowers in NC material, i.e., more Eu^{3+} ions locate in or near the particle surface, where exists a large number of

dangling bonds and disorder structures. This is also consistent with the disorder effect discussed above.

4. Conclusions

In conclusion, the energy of the charge transfer state of Eu^{3+} at the S_6 site is slightly higher than that at the C_2 site in both bulk and NC $\text{Y}_2\text{O}_3:\text{Eu}^{3+}$. CTBs of Eu^{3+} at both S_6 and C_2 sites are shifted toward lower energy in NC sample. The host prefers transferring the excitation to the Eu^{3+} ions at S_6 site, instead of C_2 site. Comparing with the bulk one, the number ratio of the S_6 sites to the C_2 sites in NC is decreased remarkably. It is attributed to the increase of disorder on the surface of the nanoparticles.

Acknowledgements

This work was funded by ‘One Hundred Talents Program’ from Chinese Academy of Sciences, the National Natural Science Foundation of China (Grant Nos. 50172047 and 10274083), and Cottrell College Awards from Research Corporation.

References

- [1] K.A. Franz, W.G. Kehr, A. Siggle, J. Wiieczoreck, in: B. Elvers, S. Hawkins, G. Schulz (Eds.), *Ullman's Encyclopedia of Industrial Chemistry*, vol. A15, VCH Publishers, Weinheim, Germany, 1985.
- [2] G. Blasse, B.C. Grabmaier (Eds.), *Luminescent Materials*, Springer, Berlin, 1994.
- [3] R.S. Meltzer, S.P. Feofilov, B. Tissue, H.B. Yuan, *Phys. Rev. B* 60 (1999) 14012.
- [4] M. Tanaka, T. Kushida, *Phys. Rev. B* 60 (1999) 14732.
- [5] A. Konrad, T. Fries, A. Gahn, F. Kummer, U. Herr, R. Tidecks, K. Samwer, *J. Appl. Phys.* 86 (1999) 3129.
- [6] T. Igarshi, M. Ihara, T. Kusunoki, K. Ohno, *Appl. Phys. Lett.* 76 (2000) 1549.
- [7] R. Schmechel, M. Kennedy, H. von Seggern, H. Winkler, M. Kolbe, R.A. Fischer, X.M. Li, A. Benker, M. Winterer, H. Hahn, *J. Appl. Phys.* 89 (2001) 1679.
- [8] H.W. Song, B.J. Chen, H.S. Peng, J.S. Zhang, *Appl. Phys. Lett.* 81 (2002) 1776.
- [9] Z.M. Qi, C.S. Shi, W.W. Zhang, W.P. Zhang, T.D. Hu, *Appl. Phys. Lett.* 81 (2002) 2857.
- [10] Y.Q. Zhai, Z.H. Yao, S.W. Ding, M.D. Qiu, J. Zhai, *Mater. Lett.* 57 (2002) 2901.
- [11] W.W. Zhang, W.P. Zhang, P.B. Xie, M. Yin, H.T. Chen, L. Jing, Y.S. Zhang, L.R. Lou, S.D. Xia, *J. Colloid Interf. Sci.* 262 (2003) 588.
- [12] T. Tomiki, J. Tamashiro, Y. Tanahara, A. Yamada, H. Fukutani, T. Miyahara, H. Kato, S. Shin, M. Ishigame, *J. Phys. Soc. Jpn.* 55 (1986) 4543.
- [13] L. Brus, *J. Phys. Chem.* 90 (1986) 2555.
- [14] H.E. Hoefdraad, *J. Solid State Chem.* 15 (1975) 175.